Structural anomalies in hcp metals under pressure: Zn and Cd

2004 J. Phys.: Condens. Matter 16 6405

(http://iopscience.iop.org/0953-8984/16/36/007)

INSTITUTE OF PHYSICS PUBLISHING JOURNAL OF PHYSICS: CONDENSED MATTER

J. Phys.: Condens. Matter **16** (2004) 6405–6414 PII: S0953-8984(04)78488-X

Structural anomalies in hcp metals under pressure: Zn and Cd

S L Qiu[1], **F Apostol**[1] **and P M Marcus**[2]

[1] Department of Physics, Alloy Research Center, Florida Atlantic University, Boca Raton, FL 33431-0991, USA
[2] IBM Research Division, T J Watson Research Center, Yorktown Heights, NY 10598, USA

Received 28 March 2004
Published 27 August 2004
Online at stacks.iop.org/JPhysCM/16/6405
doi:10.1088/0953-8984/16/36/007

Abstract

First-principles total-energy calculations with WIEN2k using a procedure that finds the equilibrium states of hcp structures under pressure from minima of the Gibbs free energy have found a structural anomaly in hcp Zn and in hcp Cd under pressure. The calculated small but definite anomaly in the pressure dependences of the structural parameters of hcp Zn allows a reinterpretation of the data to show the anomaly. We find a similar but stronger anomaly in Cd than in Zn. The calculated anomaly in Zn contradicts a recent theoretical conclusion that found that the anomaly disappears at a large number of k-points in the Brillouin zone. The calculation also shows that the uncertainty in locating equilibrium found in another recent paper is absent here. Reasons are given for computational differences from previous work. Evaluation of the pressure dependence of various elastic quantities which are much more sensitive to the anomaly shows the anomalies in hcp Zn and hcp Cd exist over a considerable range of pressure; several abrupt changes in the electron distribution are thereby indicated in that pressure range.

1. Introduction

In a recent letter [1] reporting a first-principles calculation on hcp Zn and hcp Fe we revised the previous experimental and theoretical opinions that the existence of the structural anomaly in hcp Zn under pressure is doubtful. The calculated structural anomalies as a function of pressure were shown to fit the more recent data (2002) of Takemura *et al* [2–4] and both theory and experiment show a small but definite anomaly at about 100 kbar. Calculations at both low and high k-point density in the irreducible wedge of the Brillouin zone (IBZ) show the anomaly is present at both densities without significant change. This conclusion contradicts the results of a recent first-principles calculation [5] that found the anomaly disappeared at high k-point density.

The present paper provides additional information about the results on hcp Zn and gives similar information for hcp Cd. The additional material includes the earlier structural data (1995) of Takemura [6] on hcp Zn, which has a poorer fit to the theory, includes an explicit comparison of structural parameters at low and high k-point density for both Zn and Cd, and extends the pressure range to give more perspective on the ranges of the large anomalies in elastic quantities. The same structural quantities are given for hcp Cd, where the theory does not fit the 1997 data of Takemura [7] for hcp Cd as well as the theory fitted the 2002 data on hcp Zn. The anomaly in Cd is shown to be larger and to have more structure than in Zn.

Although the anomaly in the structural parameters is small for both Zn and Cd, the elastic quantities k_c/k_a (the ratio of linear compressibilities) [8] and c_{66} show much larger effects and that the anomalies extend over a range 60–80 kbar.

The parameters of the first-principles calculation and the procedure for determining equilibrium at each pressure are given in section 2. The results of calculation are described in section 3. Section 4 discusses and evaluates the results and notes where this calculation differs from previous calculations.

2. Procedures

First-principles calculations on hcp Zn and hcp Cd under hydrostatic pressure were performed using the WIEN2k package [9], which is an implementation of the full-potential augmented-plane-wave plus local orbital (APW + lo) method together with the Perdew–Burke–Ernzerhof generalized-gradient-approximation (PBE-GGA). The APW + lo method expands the Kohn–Sham orbitals in atomic like orbitals inside the atomic spheres and plane waves in the interstitial region. The details of the method have been described in the literature [9–11]. A plane-wave cutoff $R_{\mathrm{MT}}K_{\max} = 7$, $R_{\mathrm{MT}} = 1.6$ au, $G_{\max} = 14$ and mixer $= 0.05$ were used in all the calculations. To check the negative results of [5] we used 5300 k-points in the IBZ in both the free energy and the elastic constant calculations for Zn, and for comparison, we also carried out the free energy calculations using 550 k-points in the IBZ. Similar comparison was also made for hcp Cd. The k-space integration was done by the modified tetrahedron method [9]. Tests with larger basis sets and different Brillouin-zone samplings yielded only very small changes in the results. The convergence criterion on the energies is set at 1×10^{-3} mRyd/atom.

The details of the procedure for finding the equilibrium states and the elastic constants of the hcp lattice are given in our previous reports [12]. Briefly, the equilibrium state is found from the thermodynamic result that at a given pressure p the Gibbs free energy (at zero temperature) $G \equiv E(a, c) + pV(a, c)$ is a minimum with respect to both the hcp structure parameters a and c, where E is the energy/atom and V the volume/atom. The double minimum is conveniently found from a minimum of G along the epitaxial Bain path (EBP) modified for finite pressure [12–14]. The elastic constants are then found as second strain derivatives of G in the equilibrium state at p, while p remains constant. This procedure finds the structural parameters and elastic constants directly as functions of p.

The pV term, which distinguishes G from E (at 0 K), makes an important contribution to the stress in a state of a system under applied pressure p. In a state of a homogeneous crystal at p the strain derivatives of the energy density E/V give the total stress, which includes the applied pressure; the total stress also includes other contributions when the system is strained away from the equilibrium at p. The stress from strain derivatives of pV give a pressure term that cancels the pressure included in the total stress. Hence the strain derivatives of the free energy density G/V give just the deviations of the total stress from the applied pressure, e.g., for a strained tetragonal or hexagonal crystal $\sigma_c = \frac{c}{V}(\frac{\partial E}{\partial c})_a$ is the total stress in the c direction

including a contribution of $-p$, but $\frac{c}{V}(\frac{\partial pV}{\partial c})_{a,p} = +p$ which cancels the $-p$. Hence $\frac{c}{V}(\frac{\partial G}{\partial c})_{a,p}$ is the deviation of the stress in the c direction from the applied pressure. Thus G acts for a system under finite pressure p, the same way that E acts at $p = 0$; i.e. for both E and G the gradient of the deviation of the stress for a system strained from equilibrium provides the driving force in the equations of motion that returns the system to equilibrium, i.e. to a minimum of E at $p = 0$ and to a minimum of G at finite p. As p changes the system moves through a sequence of equilibrium states which form a path along which the system properties are functions of just one variable, which could be p or V. The appendix derives relations between changes in the structural parameters and the elastic constants along the equilibrium path, one of which is used later.

3. Results

Figures 1(a)–(c) show, respectively, the lattice constants a, c and the ratio c/a of hcp Zn as functions of pressure p in the range from 0 to 140 kbar. The open diamonds are the experimental data of Takemura [6] in 1995 showing a large structural anomaly in the vicinity of 120 kbar of hydrostatic pressure. The solid diamonds are the experimental results of Takemura *et al* [2–4] in 1999 and 2002 using a better pressure medium showing a smaller anomaly around 100 kbar of hydrostatic pressure. The open circles and crosses (using 5300 and 550 k-points in the IBZ, respectively) are the theoretical results of this work showing that the anomaly is a small but definite effect on the lattice constants, which occurs in the same pressure range and has the same magnitude as the latest experimental measurement. However, figures 2(a) and (b) show that the anomaly has a large effect on the ratio of linear compressibilities $k_c/k_a = (c_{11} + c_{12} - 2c_{13})/(c_{33} - c_{13})$. (This useful formula is given in [8] without derivation or reference to a derivation. The related formula (A.6) appears in [15] without derivation. The Gibbs free energy formulation of equilibrium permits a derivation which shows the formulas are valid at all pressures; see appendix formula (A.5).) The anomaly also has a large effect on the elastic constant c_{66} in the vicinity of 100 kbar. Figure 2(c) shows the value of $G - G_0$ of hcp Zn at its minimum as a function of pressure, where G_0 is the value for hcp Zn at 0 kbar.

Reference [5] found that the calculated anomaly in lattice parameters of hcp Zn under compression exists at 732 k-points, but disappears at 5208 k-points in the IBZ. To check this finding we have performed EBP calculations using the Gibbs free energy with 5300 (open circles) and 550 k-points (crosses) in the IBZ which are shown in figures 1(a)–(c). The comparison shows no significant change in $a(p)$, $c(p)$ and $(c/a)(p)$ in the pressure range of the anomaly of hcp Zn with the change in number of k-points in the IBZ.

Figures 3(a)–(c) show, respectively, the lattice constants a, c and the ratio c/a of hcp Cd as functions of pressure p in the range from 0 to 240 kbar. The open diamonds are the experimental data of Takemura [7] showing the slope changes in the vicinity of 60 and 120 kbar of hydrostatic pressure. The open circles and crosses (using 550 and 5300 k-points in the IBZ, respectively) are the theoretical results of this work showing that the theoretical anomaly occurs in the same pressure range as the experimental measurement. The comparison between 550 and 5300 k-points in the IBZ shows no significant change with k-point density in $a(p)$, $c(p)$ and $(c/a)(p)$ in the pressure range of the anomaly of hcp Cd.

Figures 4(a) and (b) show that the anomaly has a large effect for hcp Cd on the ratio of linear compressibilities and a moderate effect on the elastic constant c_{66} in the same pressure range as the structural anomalies. Figure 4(c) shows the value of $G - G_0$ of hcp Cd at its minimum as a function of pressure, where G_0 is the value for hcp Cd at 0 kbar.

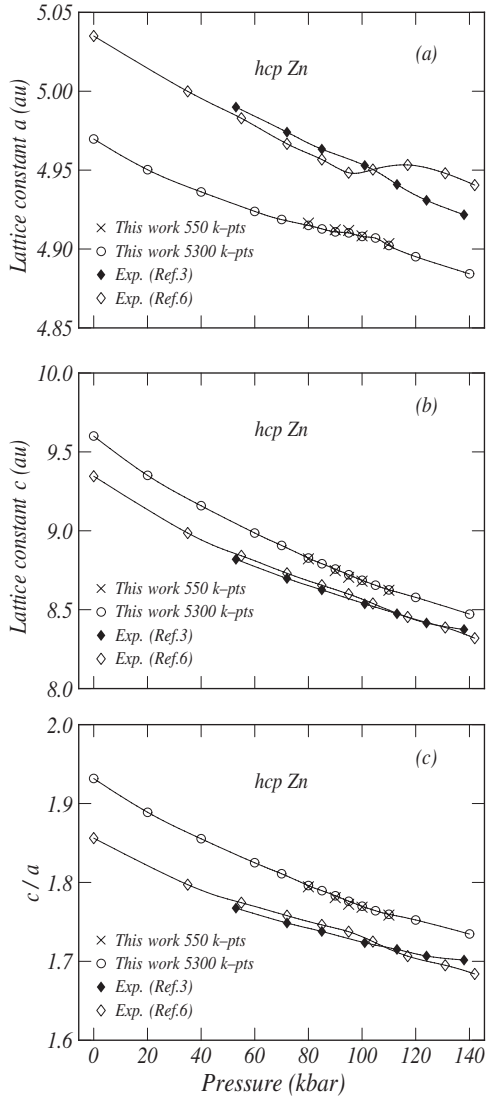

Figure 1. (a) The lattice constants a, (b) the lattice constant c and (c) the ratio c/a of hcp Zn as functions of pressure p. The solid and open diamonds are the experimental data from [2] and [6] respectively, the open circles and crosses (using 5300 and 550 k-points in the IBZ, respectively) are the theoretical results of this work. The solid curves interpolate between the data points.

Figure 5 shows the comparison of the structural anomalies between hcp Zn (open circles) and hcp Cd (solid circles) in (a) the lattice constants a, (b) the lattice constant c and (c) the ratio c/a as functions of pressure p. The insets show the anomaly in hcp Zn on expanded scales.

Figure 6 shows that the minima of G along the EBP at pressures that include the range of the anomaly have well-defined minima in contrast to the results in [16, figure 10].

4. Discussion

As evidence of the reliability of our calculation we note that the initial linear decrease of c/a as a function of pressure up to 40 kbar fits experiment well for hcp Zn as shown in figure 1(c). This verification of the initial decrease in anisotropy under pressure is a basic feature of the structure, separate from the small anomalies.

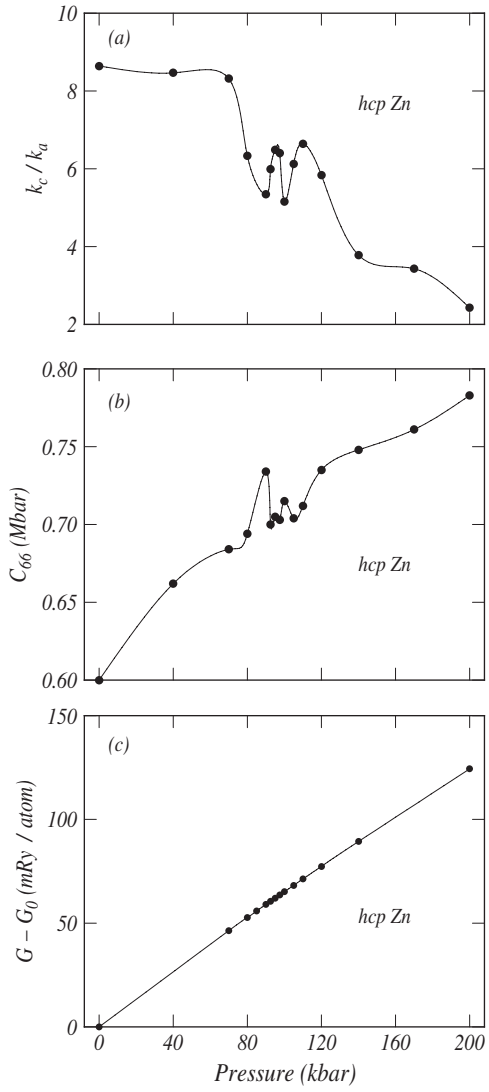

Figure 2. (*a*) The linear compressibility ratio k_c / k_a and (*b*) the elastic constant c_{66} of hcp Zn as functions of pressure p. (*c*) Free energy difference $G - G_0$ of hcp Zn as a function of pressure, where G_0 is the free energy of hcp Zn at $p = 0$. The solid curves interpolate between the data points.

The first evidence for the anomaly in hcp Zn is the rise and fall of the theoretical lattice parameter $a(p)$ forming an upward jog as p increases in the vicinity of 100 kbar (figure 1(*a*) and the inset in figure 5(*a*)). The jog is small but definite, and corresponds well in pressure range and magnitude to the small jog in the helium data in [4], whereas the theoretical jog clearly does not fit the earlier data in [6].

The comparison of theory and experiment in figure 1 is facilitated by the fact that pressure is the primary variable at which lattice constants are measured, and the theory gives the lattice constants directly as functions of pressure. When the theory gives lattice parameters as functions of volume, as previous calculations [5, 8, 16, 17] gave, the comparison of theory and experiment requires use of the equation of state $p(V)$ and incorporates the uncertainties in that function obtained by differentiating $E(V)$. The combination of theory in the present work and the helium data [2–4] provide a strong case for the existence of the anomaly.

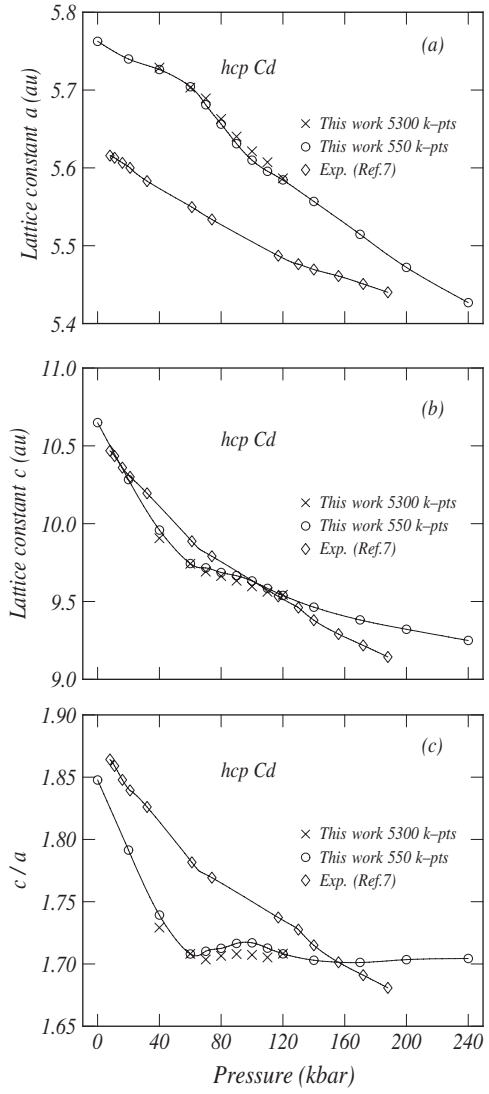

Figure 3. (*a*) The lattice constants a, (*b*) the lattice constant c and (*c*) the ratio c/a of hcp Cd as functions of pressure p. The open diamonds are the experimental data from [7], the solid circles and crosses (using 550 and 5300 k-points in the IBZ, respectively) are the theoretical results of this work. The solid curves interpolate between the data points.

The existence of the anomaly in hcp Zn is established without doubt by the remarkably large magnitudes and extended pressure range of the oscillations in elastic quantities plotted in figure 2, i.e. the linear compressibility ratio k_c/k_a and the elastic constant c_{66}. Apparently four to six abrupt electronic transitions take place over a range of at least 60 kbar. By extending the pressure range compared to [1], figure 2 shows smooth behaviour outside the limited range of the anomaly.

The effect of increasing the k-point density in the IBZ from 550 to 5300, shown in figure 1 for hcp Zn and figure 3 for hcp Cd, is small and the anomaly is clearly seen in both calculations. We feel that this correspondence of the jogs in both calculations restores confidence in structural results obtained with just a few hundred k-points in the IBZ, as is the usual case. We note that [5] states (page 2, left) that at the k-point density of 5208 k-points in the IBZ 'the anomaly in c/a has disappeared'. Additional differences between the present calculations and those of [5] and of the earlier theoretical first-principles paper of Novikov *et al* [16] concern the occurrence of

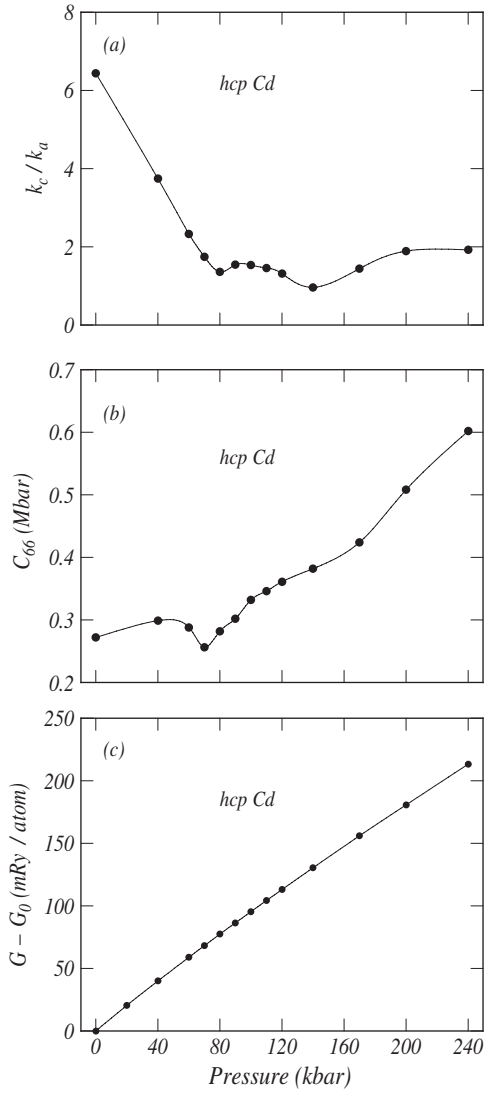

Figure 4. (*a*) The linear compressibility ratio k_c/k_a, (*b*) the elastic constant c_{66} and (*c*) free energy difference $G - G_0$ of hcp Cd as a function of pressure, where G_0 is the free energy of hcp Cd at $p = 0$. The solid lines interpolate between the data points.

minima in $a(p)$ or $a(V)$ as pressure increases or volume decreases. Thus figure 5 of [5] shows $a(V)$ has a minimum for Zn at 762 k-points in the IBZ, which is not present at 5208 k-points. Figure 7 of [16] shows that $a(V)$ has two minima. Our calculations and the experimental data do not show any minima in $a(p)$. Another difference from [5] and [16] is that [5] uses a muffin-tin radius R_{MT} of 2.0 au for Zn and [16] uses $R_{\mathrm{MT}} = 2.45$ au for Zn and 2.75 for Cd. At these values of R_{MT} we found 'ghost bands', i.e. spurious energy bands produced by using over too great a range the approximation which linearizes the energy dependence of the matrix elements of the Kohn–Sham Hamiltonian. Filling these bands with electrons would produce errors in the total energy. To remove the ghost bands we reduced R_{MT} to 1.6 au for both Zn and Cd at the cost of greater computation time. Warnings about ghost bands are given in the publications in [9]. References [5] and [16] do not mention ghost bands.

The pressure dependences of a, c and c/a of hcp Cd in figure 3 show distinct anomalies which match the trend and pressure values of the experimental data [7], but the theoretical

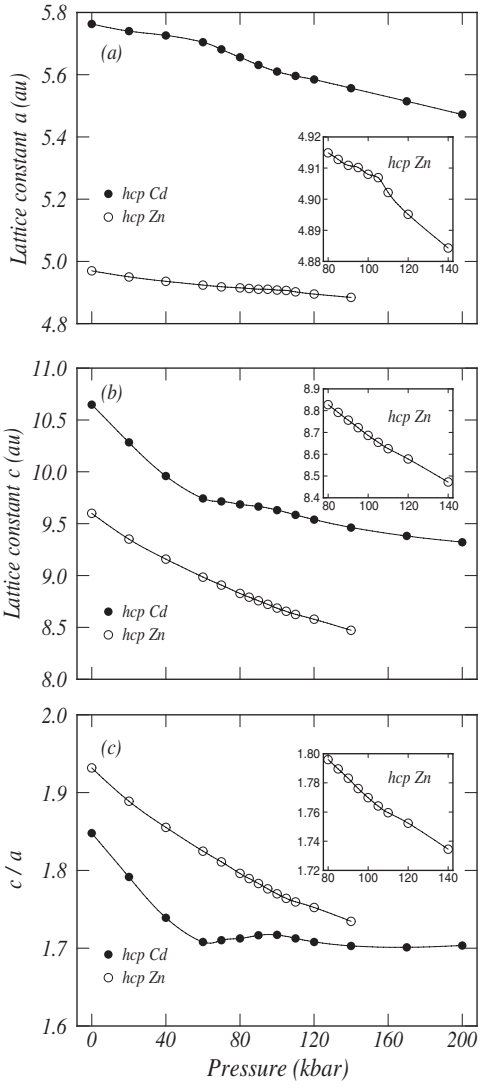

Figure 5. Comparison of the structure anomalies between hcp Zn (open circles) and hcp Cd (solid circles) in (*a*) the lattice constants a, (*b*) the lattice constant c and (*c*) the ratio c/a as functions of pressure p. The insets show the anomaly of hcp Zn on expanded scales.

anomalies are larger in magnitude. The conclusion that the anomaly exists is reinforced by the theoretical curves. We note that the observed linear decrease in anisotropy up to 60 kbar shown by c/a in figure 3(c) is in reasonable agreement with the theoretical values, although not as good as the agreement for Zn in figure 1(c); the theory levels more rapidly than experiment for Cd. This agreement for the initial linear decrease is evidence for the validity of the theory apart from the details of the anomaly.

In both [5] and [16] the procedure for finding equilibrium states is to find the minimum of $E(c/a)$ at constant V; the pressure corresponding to V is found from the equation of state $p(V)$. In the Cd calculations in [16] a difficulty with this procedure appeared which makes the theoretical results for $(c/a)(p)$ uncertain. Reference [16] finds that $E(c/a)$ in the range of the anomaly has a flat bottom or a double-well bottom (their figure 10) so that the c/a of equilibrium cannot be accurately determined. The uncertainty ranges for Cd shown in their figure 8 could contain the $(c/a)(p)$ curve in our figure 3(c) with its shallow minimum. The

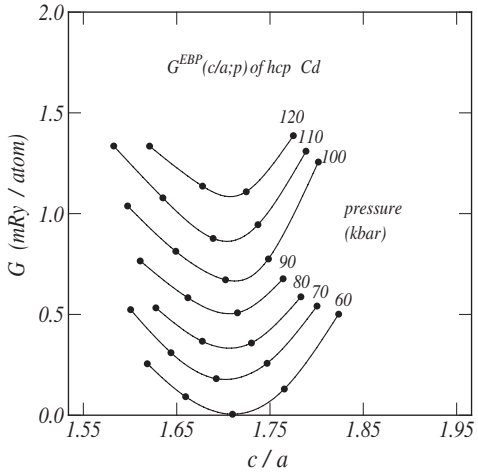

Figure 6. Gibbs free energy $G(c/a)$ of hcp Cd along the EBP at a series of pressures covering the anomalous range. For compact presentation, the minimum energy of the $G(c/a)$ curve at $p = 60$ kbar is set to zero and the $G(c/a)$ curves at pressures from 70 to 120 kbar are shifted toward zero by 9, 18, 27, 36, 45 and 53 mRyd/atom, respectively.

procedure used in our calculation for Cd from the minima of G with respect to both a and c at constant p gives a well-defined equilibrium state. Figure 6 shows the well-defined minimum at each p for Cd, in contrast with figure 10 of [16].

The elastic quantities of hcp Cd in figure 4 k_c/k_a and c_{66} show strong anomalous behaviour at about the same pressure values in a plot from 40 to 200 kbar. The k_c/k_a values show linear decrease of anisotropy from a large value of 6.4 at $p = 0$ to isotropy with $k_c/k_a \cong 1$ at about 80 kbar.

A conclusion from the numerous oscillations in $k_c/k_a(p)$ and $c_{66}(p)$ in hcp Zn and hcp Cd is that several abrupt changes take place in the electron distribution over the pressure range in which anomalies occur. The nature of these changes should be revealed by examining closely the electron distributions in this restricted range; these distributions are implicit in the calculation.

Finally we note that we have given three reasons which may account for computational differences in this work from previous work, i.e. avoidance of the equation of state to fix the pressure, avoidance of poorly defined minima for location of equilibrium, and avoidance of ghost bands.

Acknowledgments

The calculations were carried out using the computational resources BOCA4 Beowulf at Charles E Schmidt College of Science, Florida Atlantic University. P M Marcus thanks IBM for providing facilities as an Emeritus member of the Thomas J Watson Research Center. We thank K Takemura for providing his data on hcp Zn under pressure.

Appendix. Relations between structural changes and elastic constants along the equilibrium path

The minimization of $G(a, c; p)$ with respect to a and c at a given p gives the equilibrium functions $a(p)$, $c(p)$. The change in the function $G(a, c; p)$ at a given p around equilibrium

for strains that preserve hexagonal symmetry can be expanded in strains $\varepsilon_1 = \varepsilon_2 = \delta a/a$, $\varepsilon_3 = \delta c/c$ in the form

$$\frac{\delta G}{V_0} = \frac{c_{11}}{2}(\varepsilon_1^2 + \varepsilon_2^2) + \frac{c_{33}}{2}\varepsilon_3^2 + c_{12}\varepsilon_1\varepsilon_2 + c_{13}(\varepsilon_1\varepsilon_3 + \varepsilon_2\varepsilon_3), \tag{A.1}$$

where V_0 is the equilibrium volume of the unit cell. The shear strains ε_4, ε_5, ε_6, which break hexagonal symmetry, are put to zero, since pressure preserves hexagonal symmetry.

Introducing

$$\varepsilon_V \equiv \frac{\delta V}{V_0} = \varepsilon_1 + \varepsilon_2 + \varepsilon_3 = 2\varepsilon_1 + \varepsilon_3, \tag{A.2}$$

and eliminating ε_2 and ε_3 from (A.1) gives

$$\frac{\delta G}{V_0} = \varepsilon_1^2(c_{11} + c_{12} + 2c_{33} - 4c_{13}) - 2\varepsilon_1\varepsilon_V(c_{33} - c_{13}) + \varepsilon_V^2\frac{c_{33}}{2}. \tag{A.3}$$

At a given ε_V the ε_1 that minimizes $\delta G/V_0$ is found from putting $(\partial(\delta G/V_0)/\partial\varepsilon_1)_{\varepsilon_3} = 0$, which gives the ratio $\varepsilon_V/\varepsilon_1$. This ratio corresponds to the direction the system will follow when p changes, i.e. to the direction of the equilibrium path.

Hence along the equilibrium path we have

$$\frac{\varepsilon_V}{\varepsilon_1} = \frac{c_{11} + c_{12} + 2c_{33} - 4c_{13}}{c_{33} - c_{13}}, \tag{A.4}$$

$$\frac{\varepsilon_3}{\varepsilon_1} = \frac{c_{11} + c_{12} - 2c_{13}}{c_{33} - c_{13}} = \frac{\partial \ln c/\partial p}{\partial \ln a/\partial p} = \frac{k_c}{k_a}, \tag{A.5}$$

$$\frac{\varepsilon_3 - \varepsilon_1}{\varepsilon_V} = \frac{c_{11} + c_{12} - c_{13} - c_{33}}{c_{11} + c_{12} + 2c_{33} - 4c_{13}} = \frac{\partial \ln(c/a)}{\partial \ln V}. \tag{A.6}$$

The relation (A.5) is used in section 3 and figures 2 and 4—it is given in [8]; the relation (A.6) is used in [15].

References

[1] Qiu S L and Marcus P M 2003 *J. Phys.: Condens. Matter* **15** L755
[2] Takemura K 1999 *Phys. Rev.* B **60** 61710
[3] Takemura K, Yamawaki H, Fujihisa H and Kikegawa T 2002 *J. Phys.: Condens. Matter* **14** 10563
[4] Takemura K, Yamawaki H, Fujihisa H and Kikegawa T 2002 *Phys. Rev.* B **65** 132107
[5] Neumann G-S, Stixrude L and Cohen R E 2001 *Phys. Rev.* B **63** 054103
[6] Takemura K 1995 *Phys. Rev. Lett.* **75** 1807
[7] Takemura K 1997 *Phys. Rev.* B **56** 5170
[8] Fast L, Ahuja L, Nordström L, Wills J M, Johansson B and Eriksson O 1997 *Phys. Rev. Lett.* **79** 2301
[9] Blaha P, Schwarz K, Madsen Kvasnicka G D and Luitz J 2001 *WIEN2k An Augmented Plane Wave + Local Orbitals Program for Calculating Crystal Properties* ed K Schwarz Technical Universität Wien, Austria (ISBN 3-9501031-1-2)
Blaha P, Schwarz K and Sorantin P 1990 *Comput. Phys. Commun.* **59** 399
[10] Madsen G, Blaha P, Schwarz K, Sjöstedt E and Nordström L 2001 *Phys. Rev.* B **64** 195134
[11] Schwarz K, Blaha P and Madsen G 2002 *Comput. Phys. Commun.* **147** 71
[12] Qiu S L and Marcus P M 2003 *Phys. Rev.* B **68** 054103
[13] Marcus P M, Ma H and Qiu S L 2002 *J. Phys.: Condens. Matter* **14** L525
[14] Ma H, Qiu S L and Marcus P M 2002 *Phys. Rev.* B **66** 024113
[15] Neumann G-S, Stixrude L and Cohen R E 1999 *Phys. Rev.* B **60** 791
[16] Novikov D L, Freeman A J, Christensen N E, Svane A and Rodriguez C O 1997 *Phys. Rev.* B **56** 7206
[17] Li Z and Tse J S 2000 *Phys. Rev. Lett.* **85** 5130